TUNNELING IN SURFACE DIFFUSION

Assa Auerbach, Karl F. Freed and Robert Gomer
The James Franck Institute and Department of Chemistry
The University of Chicago
Chicago, Illinois 60637, U.S.A.

ABSTRACT. A description is provided of experimental data for tunneling diffusion of atoms on single crystal planes as obtained using field emission-fluctuation spectroscopy. A focus is made upon the significantly weaker than anticipated isotope effect for H/W(110) tunneling diffusion and on the coverage dependence which suggests an influence of the nuclear statistics on the diffusion. A unified analysis of both the tunneling and thermally activated regions provides insight into the nature of the interactions between the adsorbed hydrogen atom and the tungsten lattice, and these interactions, in turn, provide an explanation of the observed anomolous isotope effect for diffusion of H/W(110).

INTRODUCTION

This paper presents some experimental results of tunneling diffusion of light adsorbates on metal surfaces as measured by the fluctuation method. We then discuss the implications of these results, particularly the smallness of the observed isotope effect and present theoretical approaches to understanding the experiments.

FLUCTUATION METHOD

The experimental method [1] requires a brief description. It takes advantage of the very high linear magnification (10^5 - 10^6) of the field emission microscope in which an electron emission map of a hemispherical single crystal surface is projected onto a fluorescent screen [2]. The projected surface consists of regions of varying orientation and some well developed flats, corresponding to low index planes. Emission is exponentially dependent on work function and the latter in turn on adsorbate coverage.

By cutting a small hole in the screen it is possible to examine emission from a region of 50-100 Å in linear dimension, involving a single crystal plane. If the emitter is uniformly covered with adsorbate and then kept at a temperature where diffusion occurs, small fluctuations in emission current from the probed region can be

J. Jortner and B. Pullman (eds.), Tunneling, 281–295.

observed, corresponding to fluctuations in the number of adsorbed atoms diffusing into and out of the probed region. Measurements may be made of the time autocorrelation function f_i of the current fluctuations which are simply related to the fluctuation in the number $\delta n(t)$ of adsorbed atoms in the probed region. For a circular probed region of radius r_o and area A a natural time scale is provided by

$$\tau_o = r_o^2/4D. \tag{1}$$

The number autocorrelation function f_n is given by

$$f_n(t) = \langle \delta n(0)\delta n(t). = \frac{\langle(\delta n)^2\rangle}{A} \int_A d^2\vec{r} \int_A d^2\vec{r}', \frac{\exp[-|\vec{r}-\vec{r}'|^2/4Dt]}{4\pi Dt} \tag{2}$$

and can easily be expressed in units of t/τ_o. This is equally true of the actually measured quantity $f_i(t) = \langle \delta i(0)\delta i(t)\rangle/\langle i\rangle^2$ with $\delta i(t)$ the tunneling current, so that a comparison of the experimental function with the theoretical one yields τ_o and thus, to the accuracy of the experiment, in the determination of r_o and D. The experiments can then be repeated at different temperatures and coverages.

If the probed region has the form of a long narrow rectangular slit of dimensions 2a x 2b with b >> a and if the slit is aligned along the principal axes of the diffusion tensor (say, with the 2a dimension parallel to the x direction), it can be shown [3] that the correlation function decomposes into a product of two one-dimensional ones $f(t/\tau_x)f(t/\tau_y)$, each with its own relaxation time given by

$$\tau_x = a^2/D_{xx} \tag{3a}$$

$$\tau_y = b^2/D_{yy}, \tag{3b}$$

where D_{xx} is the component of the diffusion tensor along the x direction. Unless $D_{yy} >> D_{xx}$, the decay of the function $f(t/\tau_x)$ is so much faster than that of $f(t/\tau_y)$, and consequently only D_{xx} is measured. Rotation of the slit by 90^o then allows measurement of D_{yy}.

The resolution of the field emission microscope is λ = 30-40Å [2], which can be comparable to the narrow dimension of a rectangular probe. However, this complication can be handled straightforwardly. In essence, the result is an increase in the effective probe dimensions by an additive amount $\sim 0.75\lambda$ [4].

The fluctuation method requires for its implementation fields of the order of 0.3-0.5 volt/Å. Adsorbates with high polarizability α and/or high dipole moment μ have their activation energies (or barrier heights) at these fields differ from those at zero field by

$$\Delta E = (1/2)\alpha(F_s^2 - F_o^2) + \vec{\mu}\cdot(\vec{F}_s - \vec{F}_o), \tag{4}$$

where F_s and F_o are the fields experienced by the ad-particle at saddle points and stable binding sites respectively. The effects for adsorbates like H, O and CO are essentially negligible, particularly on close packed planes where $F_s/F_o \sim 1$. It can also be demonstrated experimentally that the field emission current seems to have no effect on diffusion over at least two orders of magnitude, the experimentally accessible range [5].

RELATION OF D TO MICROSCOPIC QUANTITIES

The diffusion coefficient D, which is measured by the fluctuation method, is the Fick's law, or "chemical", rather than the single atom displacement or tracer diffusion coefficient D^*. D and D^* differ from each other except at zero coverage, and the relation between them is not analytically accessible except for the simplest kind of interaction, i.e., delta function repulsion which produces site exclusion. Direct and substrate mediated adsorbated-adsorbate interactions enter in a complicated way into the determination of the tracer coefficient D^* and in even more complicated ways into D.

Both D and D^* are often forced into the form

$$D = a^2 \nu P, \tag{5}$$

where a is a mean jump length and νP an effective jump frequency; ν can be thought of as an attempt frequency and P an effective jump probability. In thermally activated diffusion P is a Boltzmann average which is complicated because the actual activation energies for a given jump vary with local adsorbate configuration because of ad-ad interactions. (Incidentally, the same seems to be true of ν as well as for hydrogen on W(110).) In tunneling diffusion P is a similarly weighted tunneling probability. Thus the connection between an overall D and individual atomic events is not as direct as might be hoped. (D^* cannot be measured presently, except on the computer.) An important aid in interpretation is provided by computer simulations, even at the Monte Carlo level, where P and ν can be assigned values based on local ad-ad configurations and interaction energies both in activated and tunneling diffusion. By working backward and experimenting with various interactions in the simulation or by calculating microscopic jump rates theoretically, a fit to experiment can then be attempted.

A simple but quite useful example of this approach is provided by diffusion anisotropy. Ratios of D^*_{xx}/D^*_{yy} can be calculated for any surface structure if the actual jump directions are known and if all ad-ad interactions leave the surface symmetry intact. It then turns out, both from Monte Carlo simulations and from quasi-analytical theory [6] that

$$D^*_{xx}/D^*_{yy} = D_{xx}/D_{yy}, \tag{6}$$

so that a measurement of anisotropy can often be interpreted straightforwardly

TUNNELING DIFFUSION

We now present experimental results for the diffusion of hydrogen and its isotopes ($^mH, m = 1,2,3$) on the W(110) plane of tungsten [5]. Figure 1 shows plots of log D vs. 1/T for ^1H. Similar sets of curves are found for ^2H and ^3H. The data exhibit two markedly different temperature regimes, a thermally activated region above 140K and a rather temperature independent one between 27K and 140K with a rather sharp crossover between them. Analysis of the data in the thermally activated regime produces activation energies of 5-6 Kcal/mole, depending on coverage and very slightly on mass. This section concentrates on the temperature independent regime, while the following one considers some aspects of the thermally activated range in order to provide an explanation of the low coverage data ($\theta \leq 0.1$) for both regions using the same model of the hydrogen-tungsten lattice interactions and their effects on the diffusive processes.

The temperature independent regimes cover a wide range of T in which D is also sensitively to coverage. Figure 2 shows log D vs. coverage θ for all three isotopes at 27K. θ is deduced from work function measurements and assumes the change in work function $\Delta\phi$ to vary linearly with θ. It is also believed that $\theta = 1$ corresponds to a ratio H/W = 1; this is based on relative saturation coverages on the (110) and (100) planes and absolute measurements on (100) [7].

The most striking feature of the temperature independent diffusion data is the relatively small isotope effect seen in tunneling. If we assume that D is approximately given by

$$D = a^2 \nu P, \tag{7}$$

with the typical values $a \sim 2 \times 10^{-8}$ cm, $\nu = 10^{12} - 10^{13}$ sec^{-1} and the conventional tunneling probability

$$P = \exp[-2(2m_H/\hbar^2)^{1/2} \int_{x_1}^{x_2} (V-E)^{1/2}\, dx] \tag{8}$$

$$\approx \exp[-2(2m_H/\hbar^2)^{1/2} V_0^{1/2} \ell],$$

where V_o is barrier height, m_H is the hydrogen mass and ℓ an effective barrier length which can be adjusted according to the barrier shape, we are immediately faced with a dilemma, even allowing for the fact that P is an average value (since V_o depends on ad-ad interactions and hence on the local environment of the tunneling atom): If the smallness of the isotope effect is to be explained on the basis of the ratio $m_1 : m_2 : m_3 = 1:2:3$, $V_o^{1/2}\ell$ must be extremely small, so small in fact

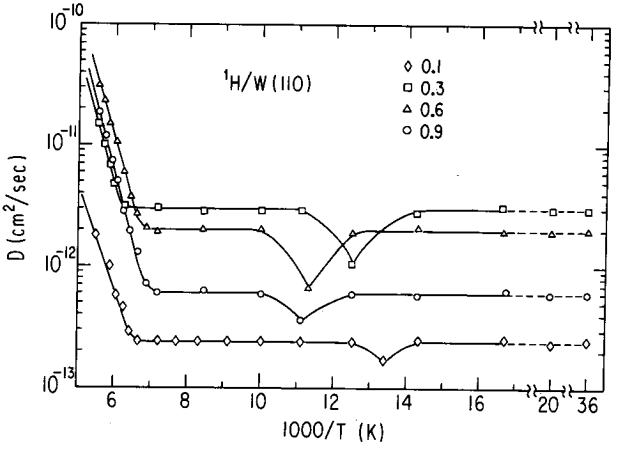

1) Log D vs.1/T for ^{1}H diffusion on W(110). Relative coverages marked on figure. The dips in the otherwise temperature independent parts result from a first order phase transition (from Ref. 5).

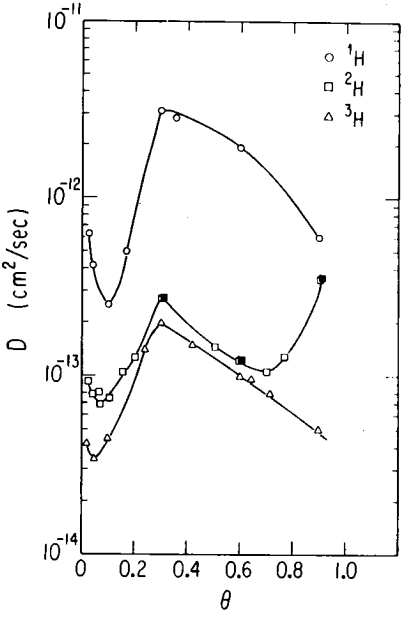

2) Log D vs. θ for ^{1}H, ^{2}H and ^{3}H at 27K (from Ref. 5).

that D with this predicted isotope effect would be some 10^6 times larger than observed unless $a^2\nu$ were smaller than $\sim 10^{-3} cm^2 sec^{-1}$ by a factor of $\sim 10^6$. If V_o is approximately given by the activation energy of thermally activated diffusion, i.e., 5-6 Kcal/mole, there is another problem: ℓ would then have to be a small fraction of an Angstrom, which seems physically unreasonable on the basis of the surface structure discussed below. We are, therefore, forced to assume that there is a contribution which enters in the form of mass renormalization, involving additive mass corrections which arise from lattice distortion by the adsorbate. This distortion accompanies the tunneling H atom and thus leads to increased effective mass. This idea was first suggested in this context by Muttalib and Sethna [8].

Analysis of Figure 2 suggests that even with this approach some difficulties remain, namely the corrections themselves must be slightly mass dependent. Figure 3 plots the product of effective mass M^* in amu times ℓ^2 in $(Å)^2$ vs. θ, assuming no change in V_o. The latter is probably an incorrect assumption, but the approximation serves to give a feeling for the magnitude of the corrections involved. The experimental data provide effective masses of all three isotopes as roughly 10-12 amu (depending on the value of $\ell \leq 0.8$ Å chosen for a triangular barrier). The next section of this paper provides attempts to explain this behavior.

The second point of note involves the coverage dependence, namely the minimum near $\theta = 0.1$ and the maximum near $\theta = 0.3$, as well as the fact that D increases again for ^2H at $\theta \geq 0.6$. The initial minimum is not well understood. It may have to do with the asymmetry of forces at low θ which leads to extra mass renormalization. Before describing attempts to explain the maximum near $\theta = 0.3$ and the differences at $\theta \geq 0.6$ between ^1H and ^3H, on the one hand, and ^2H, on the other, some anisotropy results [7] must be presented and analyzed.

Figure 4 shows a picture of the W(110) plane. If the actual jump directions are along the (111) directions labelled x_1 and x_2 in Figure 4, it can readily be seen that D^*_{110}/D^*_{100} (i.e., D^*_{yy}/D^*_{xx}) = 2. Monte Carlo calculations [6] confirm that this is so for D_{yy}/D_{xx} for any set of interactions. This result is in fact observed for oxygen on W(110) [7]. For ^1H and ^2H, however, (^3H was not available in this apparatus) it is found that $D_{110}/D_{100} \sim 1$, even in the tunneling regime at essentially all coverages, although D_{yy}/D_{xx} increases slightly at $\theta \leq 0.1$ [7]. (See Fig. 5.)

Figure 6 again shows the (110) surface with various positions labelled. It seems reasonable that 1 or 5 represent the binding sites of H with probably shallow intervening maxima at locations like 4 and the main diffusion barriers at locations like 2, 6, etc. In order to explain the observed D_{110}/D_{100} ratio, it is therefore necessary to postulate that jumps like 1→7 occur in tunneling diffusion with appreciable probability relative to "ordinary" jumps like 1→5. This suggests that most of the barrier opacity comes from the large

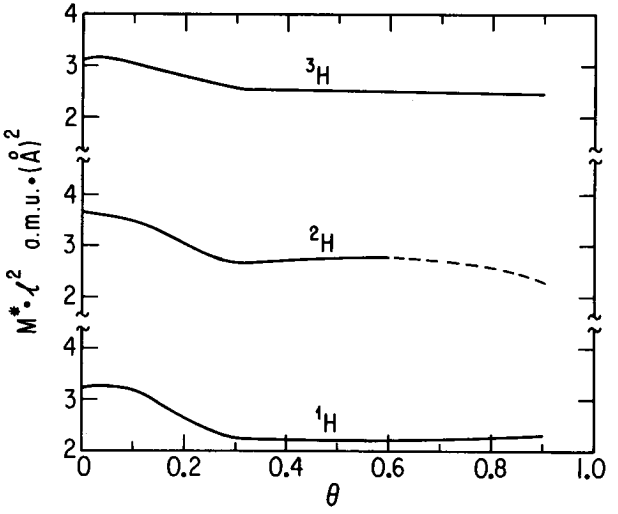

3) Effective mass M^* (in amu) times (barrier length in Å)^2, assuming constant barrier height, as function of θ for ^{1}H, ^{2}H and ^{3}H in the tunneling regime (from Ref. 5).

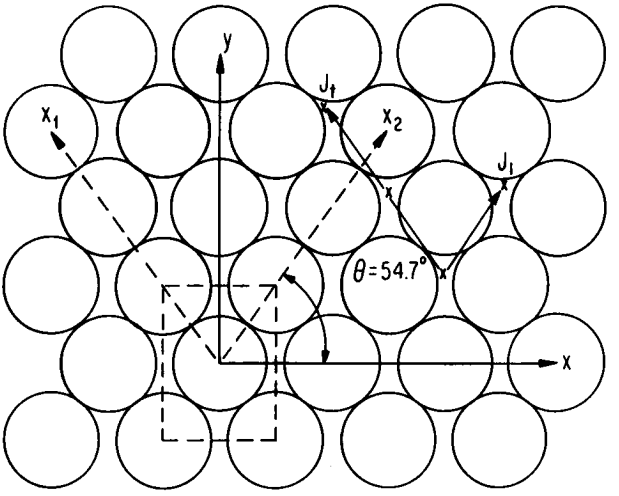

4) Schematic diagram of a (110) plane of a bcc metal. y corresponds to the (110) direction in the plane, x to the (100) direction. x_1 and x_2 correspond to (111) directions and are assumed to represent the actual jump directions in the surface diffusion. Also indicated are the nearest neighbor interaction J_1 and the linear triplet interaction J_t.

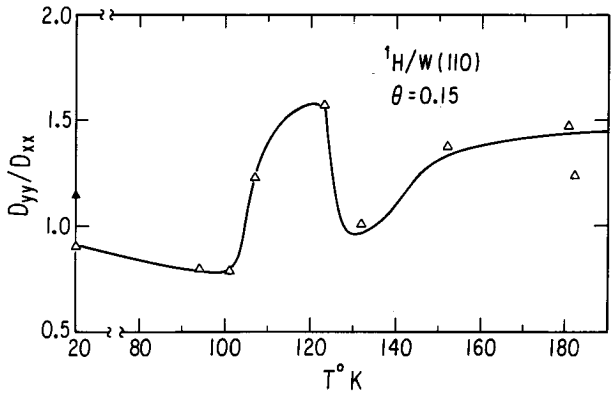

5) D_{yy}/D_{xx} for ^{2}H at θ = 0.15 as function of temperature (from Ref. 7).

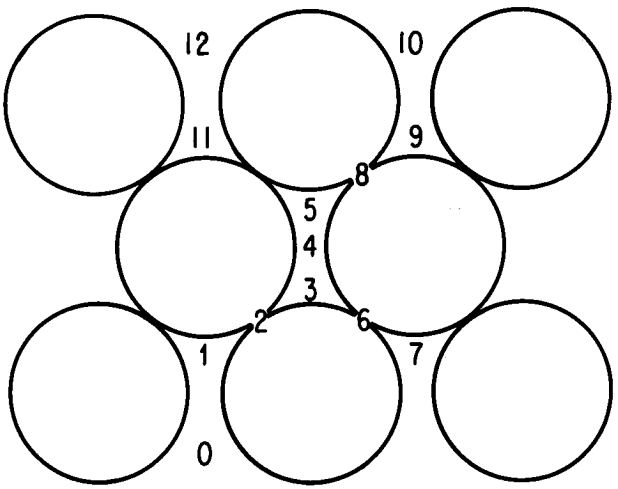

6) Schematic diagram of the (110) plane indicating possible ad-sites and diffusion barriers.

effective mass and that the contributions from integrals over phonon coordinates from events like 1→7 and 1→5 may not be too different.

A possible reason why such events occur for H diffusion is provided by the observation of Estrup [9] that hydrogen adsorption on W(110) shifts the entire top layer of W atoms along the (110) (y in Fig. 4) direction, thus removing the degeneracy of the two ends of the hour-glasses in Figs. 4 and 6 and making sites like say 1, 5 and 7 binding but 3,9, etc., non-binding. This would give a tunneling or thermally activated atom a choice on "reaching" position 3 whether to go to 5 or 7.

We consider next the behavior of ^2H at $\theta \geq 0.6$. We hypothesize that the difference between ^2H and the other isotopes at high θ has to do with nuclear spin in the following sense. If the motion of bonding electrons is much faster than that of hydrogen nuclei, the exchange of two H atoms involves only the nuclear statistics. Then adsorbed ^1H and ^3H must be regarded as spin 1/2 fermions, ^2H as a spin 1 boson. Since the spin functions are randomly oriented at and above the lowest temperature 27K used, the symmetric spin triplet has a weight of 3/4, and the antisymmetric singlet a weight of 1/4 for ^1H and ^3H. Thus the space part of the wave function is antisymmetric in 3 out of 4 encounters on average in order to obey Fermi statistics. For ^2H, on the other hand, similar reasoning shows that the space part of the wave function is symmetric in 2 out of 3 encounters. Thus two ^1H or two ^3H atoms can approach each other closely only in 1 out of 4 encounters, while two ^2H atoms can do so in 2 out of 3 cases. We now assume that tunneling from 1 to 7 is possible if site 5 is occupied, but that there is sufficient amplitude at 3 from the atom at 5 to affect the tunneling probability of an atom originally at 1. This modulation is assumed to take the form of allowing a 1→7 event only 1 out of 4 times for ^1H or ^3H, but 2 out of 3 times for ^2H.

In order to prevent D_{100}/D_{110} from exceeding unity when 1→7 events are allowed, it is additionally necessary to postulate that concerted double tunneling events occur with finite probability. Such events are assumed to consist of an initial configuration with sites 1 and 5 filled going to a final one with sites 1 empty and 5 and 10 (or 12) filled. The probability of these events is assumed to be finite relative to single tunneling events because the overall distortions involved in the double jump may be much less than that for two non-concerted events. The effect of the statistics postulated for 1→7 jumps is assumed to hold also for concerted double tunneling, i.e., it is allowed 1 out of 4 times for ^1H and ^3H and 2 out of 3 times for ^2H.

We return now to the maximum in D at $\theta = 0.3$. As indicated by Fig. 3, this could simply be the result of small changes in effective mass, but it seems unlikely that these would lead to maxima for all three isotopes at the same value of θ. It is much more likely that the variation in D with θ is due to variations in barrier height, resulting from the opposing effect of attractive and repulsive H-H interactions.

Monte Carlo simulations have been performed in which the local tunneling probability P is a function of such interactions and in which the postulated quantum statistical effects as well as jumps like 1→7

and 1→12 are included. These simulations are, in fact, able to reproduce at least qualitatively the observed behavior, namely a single maximum for ^1H and ^3H and an upturn in D for ^2H at $\theta > 0.6$ [6]. The interactions are chosen also to reproduce the observed D_{yy}/D_{xx} in the activated and tunneling regimes and to consist of repulsive nearest neighbor J_1 and attractive triplet interactions J_t. If $J_1 = 1.6$ Kcal/mole and $J_t = -2.4$ Kcal/mole, the results shown in Fig. 7 are found. These have qualitative rather than quantitative significance; they do not quite reproduce the trend in D_{yy}/D_{xx}, and they lead to a p(1x1) ground state; the latter, however, may not be in accord with the phase diagram of H/W(110) which is very incompletely known [6]. If slightly different values of J_1 and J_t are used, a different phase diagram results, the anisotropy can be matched better, the peak for ^1H and ^3H at $\theta = 0.3$ can be retained, but the primary maximum for ^2H is shifted to $\theta = 0.6$. Thus a quantitative fit to experiment is not possible with the simple models used, but the qualitative agreement suggests that both the 1→7 and double tunneling events as well as the invoked quantum statistical effects seem to be pointing in the right direction.

LATTICE-HYDROGEN INTERACTIONS AND MODELS OF TUNNELING DIFFUSION

The same interactions between the adsorbed hydrogen atom and the substrate tungsten lattice must govern the diffusion dynamics in both the tunneling and thermally activated regions. A consistent theory should, therefore, explain the data in both the tunneling and thermally activated regions. We confine attention to the limit of vanishing coverage where complications due to adatom-adatom interactions and statistics are not present. Our discussion begins with a semiquantitative explanation of some of the striking aspects of the observed data in the thermally activated regime as this provides important constraints on the new interpretation of the tunneling data which follows thereafter.

The thermally activated diffusion constant is in agreement with the Arrhenius form

$$D(T) = A(m)\exp(-\bar{V}/T), \quad \bar{V} = 185 \pm 15\text{meV}, \tag{9}$$

where m = 1, 2 or 3 for ^mH and where $\bar{V}$ is only slightly isotope dependent in a fashion consistent with small zero point energy differences. However, the prefactor A exhibits unusual exponential mass dependence which is shown in Fig. 8 to vary rather roughly as

$$A(m) \sim \exp(-30m^{-1/2}) \tag{10}$$

and which leads to the enormous inverse isotope effect wherein A(3) is approximately five orders of magnitude larger than A(1). Clearly, such a huge isotope effect must have quantum mechanical origins. [10]

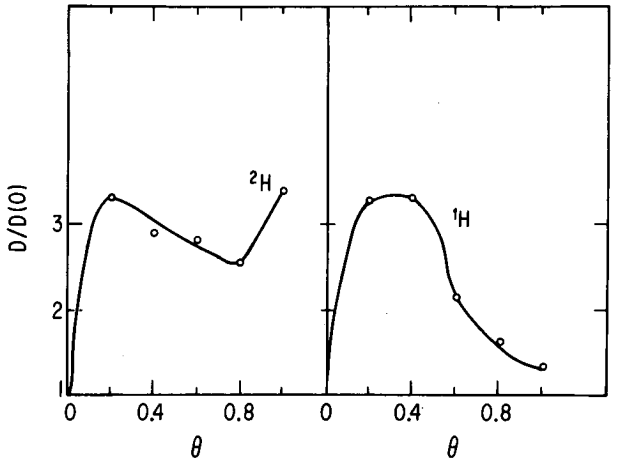

7) Monte Carlo results for D vs. θ in the tunneling regime for ^{1}H (and ^{3}H) and for ^{2}H, using the interactions and postulated events discussed in the text (from Ref. 6).

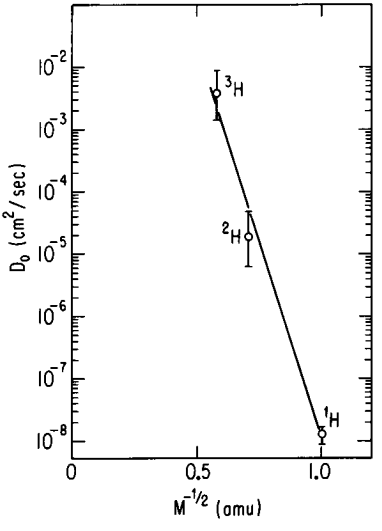

8) Data (extrapolated to θ =0) log D versus $m^{-1/2}$ with straight line designed to guide approximate fit to (11) (from Ref. 10).

An analysis has been made of the dynamics of this thermally activated diffusion by treating the activation process involved in the diffusion as occuring by a series of incoherent jumps between consecutive vibron levels for hydrogen motion in a single well [10]. This model describes a single jump as arising when energy is transfered from a highly excited local phonon mode of frequency ω_ℓ to the hydrogen adatom which is thereby promoted by a vibronic quantum of energy $\hbar\omega_H \gg \hbar\omega_\ell$ with ^mH having the frequency $\omega_{m_H} = \omega_H m^{-1/2}$. The great disparity between ω_H and ω_ℓ leads naturally to the use of an adiabatic approximation where the hydrogen motion occurs adiabatically as a function of fixed substrate lattice position q. The vibron energy $E_n(q)$ provides a contribution to the potential energy determining the slower lattice dynamics. The characteristic timescale for an activation step between the nth and n+1st vibron levels depends on the matrix element of the nonadiabatic hydrogen-tungsten coupling and on a lattice overlap factor for the local phonon mode.

This type of model calculation yields [10]

$$A^f \propto \omega_H \ell^2 \left(\frac{\omega_H}{\omega_\ell}\right)^{3/2} \exp\{-X_{01} - m^{-1/2}\left(\frac{\omega_H}{\omega_\ell}\right)\left(\ln\left[\frac{m^{-1/2}}{X_{01}}\left(\frac{\omega_H}{\omega_\ell}\right)\right]-1\right)\}, \tag{11}$$

where ℓ is the intersite distance $\sim 2\text{Å}$, m is the isotope mass in amu, and the parameter X_{01} is discussed below. (We neglect the weak m dependence in the prefactor.) The ratio ω_H/ω_ℓ equals the number of phonons needed to promote the hydrogen to a higher vibronic state, and the ratio is also measure of the degree of adiabaticty or separation of time-scales which underlies this analysis.

It is natural to assume that the vibron and local phonon motions have effective masses which are, respectively, proportional to that of hydrogen (m_H) and tungsten (m_W). Since values of ω_H/ω_ℓ deduced by comparing (11) with the experimental data yield values which are within an order of magnitude of the reduced mass ratio $(m_W/m_H)^{1/2} = 13.5$, this strongly suggests that pairwise W-W and H-W force constants of the local and vibron modes, respectively, are of similar orders of magnitudes.

The parameter X_{01} in (11) provides a measure of the quantum nature of the hydrogen-lattice forces, and it is given by [10]

$$X_{01} = (m_W\omega_\ell/2\hbar)\,(\bar{q}^{(1)} - \bar{q}^{(0)})^2 \tag{12}$$

where $\bar{q}^{(n)}$ is the position of the minimum of the adiabatic potential for the local mode with the vibron in the nth state. If the vibron contribution to this potential is $[n + (1/2)]\hbar\omega_H$, then X_{01} is proportional to m^{-1} [10]. Comparison of (11) with experimental data provides the rough estimate that X_{01} O(1). The fact that X_{01} is non-zero allows us to anticipate that the adiabatic ^mH-W local mode potentials are isotope dependent! This same kind of isotope dependence appears also to be required in order to explain the low temperature data.

The low temperature diffusion coefficient is dominated by intersite quantum tunneling. The lowest temperature of 27K is still very high compared to the measured inverse hopping time (D/ℓ^2). The energy associated with this hopping time is $\hbar D\ell^{-2} \sim 10^{-9}$eV, making it appear impossible to justify a coherent band description, such as that for electrons in metals, for the motion of the hydrogens. Thus, we are led to assume that low energy inelastic processes of energy $\Delta << 27K$ destroy the phase coherence between consecutive hops. Such processes are easily explained in terms of a coupling of the hydrogen motion to electron-hole excitation of the metals and to low lying acoustical phonons.

This model of the hydrogen tunneling implies that D is therefore described by the small polaron hopping rate. A detailed calculation by Flynn and Stoneham [11] using Holstein's treatment [12] gives in this case

$$D = \ell^2 J^2/\hbar\tilde{\Delta}\ , \tag{13}$$

where J is the transition matrix element which in a semiclassical approximation is [13]

$$J = m^{1/4}\omega_H\left(\frac{2m_H\omega_H}{\pi\hbar\ell_T^2}\right)^{1/2} \exp[-m^{1/2}S_H - S_W]. \tag{14}$$

Here S_H is the classical "action" for the hydrogen tunneling a distance ℓ_T under the potential barrier $V_H(x)$,

$$S_H = \frac{1}{\hbar}\int_{-\ell_T/2}^{\ell_T/2} [2m_H V_H(x)]^{1/2}\, dx, \tag{15}$$

and S_W is the overlap factor, discussed below in (19), which is associated with the motion that the tungsten atoms undergo due to the lattice distortion (polaron) that accompanies the hydrogen tunneling. Using a smooth potential of the form

$$V_H(x) = \bar{V}[(2x/\ell_T)^2 - 1]^2 \tag{16}$$

with values of $\bar{V}$ as in (9) and ℓ_T of order 0.5 - 0.8 Å, the magnitude of $D(^1H)$ in the limit of zero coverage (Fig. 3) is fitted by the set of parameters in the range

$$S_H \approx 3.7 \pm 0.6\ ,\quad S_W \approx 14 \pm 2, \tag{17}$$
$$\hbar\omega_H = 100\text{meV}\ ,\quad \text{and } \tilde{\Delta} \approx 0.1\text{-}2.0\ \text{meV},$$

where the large range for $\tilde{\Delta}$ leads to the quoted uncertainty in the value of S_W which is fit to experiment. However the smaller than expected isotope effect cannot be explained by the polaron model (14)

unless S_W is allowed to vary with m, so as to partially compensate for the large isotopic variations of $m^{1/2}S_H$. The required mass variation is roughly given by

$$\frac{\partial S_W(m)}{\partial m} \approx -1.5\pm0.3 \ . \tag{18}$$

Two important conclusions emerge from (17) and (18). The first is that the lattice participation in the tunneling is very large because $S_W \gg S_H$. This has earlier been described by Muttalib and Sethna [8] as a large "mass renormalization" effect, but our analysis here suggests a separation of timescales which leads to a different interpretation. Secondly, the local mode H-W force constants, which determine S_W, are influenced by the quantum motion of the hydrogen. This influence, manifested by the mass dependence of these force constants, is a natural consequence of the adiabatic approximation for the more rapid hydrogen motion.

A qualitative estimate of the magnitude of X_{01} in (12) can be made by using a model with a single linearly coupled phonon-hydrogen potential. Such a model yields

$$S_W = (m_W\omega_\ell/\hbar)\bar{q}^{(0)2} \ , \tag{19}$$

where $\bar{q}^{(0)}$ is the polaron distortion of the lattice mode which minimizes the sum of W-W and H-H potential energies. Equation (12) contains the lattice distortion $\bar{q}^{(n)}$ defined for each adiabatic vibron potential. We assume here that $\bar{q}^{(n)}$ depends solely on the harmonic vibron state, and this provides a relation between the isotope and n-dependence which is given by

$$\bar{q}^{(n)}_m = \bar{q}[(n + \tfrac{1}{2})\hbar\,\omega_H m^{-1/2}]. \tag{20}$$

(A specific example of such an interaction has been given by Emin [14].) Thus, combining (12), (19) and (20) leads to the estimate of

$$(\frac{\partial S_W}{\partial m})^2 = S_W X_{01}/4m, \tag{21}$$

which in turn gives $X_{01} \sim 0.5\text{-}2$. The latter is in accord with the estimates provided on the basis of the thermally activated diffusion data. Although (21) depends on a simplified two-dimensional model for the H-W potential, the agreement of the estimates for X_{01} from the activated and thermal data verifies the consistency of our approach and assures that the relation (20) is approximately valid.

In summary, our analysis of the data suggests a sizeable isotope dependence of the adiabatic H-W local mode potentials as well as a large participation of the lattice in the diffusion process in both the low and high temperature regimes.

We are grateful to D. Emin for a useful discussion. This research is supported by MRL(NSF) facilities at the University of Chicago.

References

[1] R. Gomer, Surf. Sci. 38, (1973) 373; G. Mazenko, J.R. Banavar, and R. Gomer, Surf. Sci. 107, (1981) 459.
[2] R. Gomer, Field Emission and Field Ionization, Harvard University Press (1960).
[3] D.R. Bowman, R. Gomer, K. Muttalib and M. Tringides, Surf. Sci. 138, (1984) 581.
[4] R. Gomer and A. Auerbach, Surf. Sci., in press.
[5] S.C. Wang and R. Gomer, J. Chem. Phys. 83, (1985) 4193.
[6] M. Tringides and R. Gomer, Surf. Sci. 166, (1986) 419; M. Tringides and R. Gomer, Surf. Sci. 166, (1986) 440.
[7] M. Tringides and R. Gomer, Surf. Sci. 155, (1985) 254.
[8] K. Muttalib and J. Sethna, Phys. Rev. B32, (1985) 3462.
[9] P. Estrup, Phys. Rev. Lett., in press.
[10] K.F. Freed, J. Chem. Phys. 82, (1985) 5264.
[11] C.P. Flynn, A.M. Stoneham, Phys. Rev. B10, (1970) 3966.
[12] T. Holstein, Ann. Phys. 8, (1959) 343.
[13] A. Auerbach and S. Kivelson, Nucl. Phys. B257, [F514] (1985) 799.
[14] D. Emin, private communication.